

Unconventional low-field magnetic response of a diffusive ring with spin-orbit coupling

Moumita Patra¹ and Santanu K. Maiti^{1,*}

¹*Physics and Applied Mathematics Unit, Indian Statistical Institute,
203 Barrackpore Trunk Road, Kolkata-700 108, India*

We report an unconventional behavior of electron transport in the limit of zero magnetic flux in a one-dimensional disordered ring, be it completely random or any correlated one, subjected to Rashba spin-orbit (SO) coupling. It exhibits much higher circulating current compared to a fully perfect ring for a wide range of SO coupling yielding larger electrical conductivity which is clearly verified from our Drude weight analysis.

PACS numbers: 73.23.-b, 73.23.Ra, 73.21.Hb

I. INTRODUCTION

The phenomenon of non-decaying circular current, the so-called persistent current, in an isolated mesoscopic ring threaded by magnetic flux ϕ was first suggested by Büttiker and his group¹ during early 80's. Following this proposal a considerable amount of theoretical work has been done²⁻¹³ towards this direction analyzing the effects of different factors like electron-electron (e-e) interaction, electron-phonon (e-ph) interaction, temperature, randomness, long-range hopping, spin-orbit (SO) couplings, etc. With these studies many significant features have been explored those are consistent with ex-

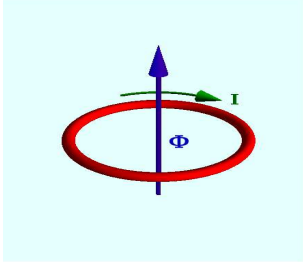


FIG. 1: (Color online). Schematic view of a 1D ring carrying a current I in presence of magnetic flux ϕ .

perimental observations¹⁴⁻¹⁹ upto a certain level. But few debates still persist. For example, the appearance of discrepancy between current amplitudes in disordered rings obtained from experimental results and theoretical estimates. Measured currents are always higher than theoretical predictions. Much efforts have been paid to resolve this issue and with some recent theoretical works possibilities of getting larger currents have been suggested which in some cases are very close to the experimental observations. The essential factors those are responsible to enhance current in disordered rings are e-e interactions³ and SO coupling¹¹. Two types of SO couplings, namely Rashba²⁰ and Dresselhaus²¹, are usually encountered in solid state materials, out of which one (Rashba term) is controlled externally²², whereas the other is material dependent. Both these two coupling terms play identical role in enhancing current in a disordered ring as they are simply connected by a unitary

transformation¹¹, and due to this reason, in our present manuscript we consider only one of them.

It is well known that a disordered non-interacting (i.e., without any e-e interaction) ring and free from any kind of SO coupling exhibits much smaller current⁶ compared to a perfect ring. This is essentially due to electronic localization. But if we include SO interaction, a sufficient enhancement of current takes place¹¹ though it is always much less compared to a perfect ring. Now all these features have been studied for moderate magnetic fluxes and, to the best of our knowledge, no one has investigated the response in the limit $\phi \rightarrow 0$. From our critical and deep analysis we find an unconventional electronic behavior of a disordered ring in the limit of zero magnetic field subjected to SO coupling. Much higher current is obtained in a disordered ring than a completely perfect one for a wide range of SO interaction, in contrast to the conventional literature knowledge. This enhancement is also reflected in electrical conductivity which we show by evaluating Drude weight.

The rest of our work is organized as follows. In Sec. II we present the model and describe briefly the theoretical prescription. The results are placed in Sec. III, and finally, we summarize in Sec. IV.

II. MODEL AND THEORETICAL FORMULATION

Figure 1 presents the schematic diagram of a one-dimensional (1D) ring threaded by a magnetic flux ϕ (measured in unit of $\phi_0 = ch/e$). The tight-binding (TB) Hamiltonian of such a N -site ring, subjected to Rashba SO coupling, reads as²³

$$\begin{aligned} \mathbf{H} = & \sum_n \mathbf{c}_n^\dagger \epsilon_n \mathbf{c}_n + \sum_n \left(e^{i\theta} \mathbf{c}_{n+1}^\dagger t \mathbf{c}_n + e^{-i\theta} \mathbf{c}_n^\dagger t^\dagger \mathbf{c}_{n+1} \right) \\ & - \sum_n \alpha \left[\mathbf{c}_{n+1}^\dagger (i\sigma_x \cos \varphi_{n,n+1} + i\sigma_y \sin \varphi_{n,n+1}) \right. \\ & \left. e^{i\theta} \mathbf{c}_n + h.c. \right] \end{aligned} \quad (1)$$

where α measures the strength of Rashba SO coupling and $\varphi_{n,n+1} = (\varphi_n + \varphi_{n+1})/2$ with $\varphi_n = 2\pi(n-1)/N$ (n is the site index). σ_x , σ_y and σ_z are conventional

Pauli spin matrices. Considering $c_{n\sigma}^\dagger$ ($\sigma = \uparrow, \downarrow$) and $c_{n\sigma}$ as the creation and annihilation operators, respectively, we construct \mathbf{c}_n and \mathbf{c}_n^\dagger and they look like

$$\mathbf{c}_n = \begin{pmatrix} c_{n\uparrow} \\ c_{n\downarrow} \end{pmatrix} \text{ and } \mathbf{c}_n^\dagger = \begin{pmatrix} c_{n\uparrow}^\dagger & c_{n\downarrow}^\dagger \end{pmatrix}. \mathbf{t} \text{ and } \boldsymbol{\epsilon}_n \text{ are both}$$

(2×2) diagonal matrices where $\mathbf{t}_{11} = \mathbf{t}_{22} = t$ (t being the nearest-neighbor hopping element and during each hopping a phase factor $\theta (= 2\pi\phi/N\phi_0)$ is introduced), and $\epsilon_{n\uparrow}$ and $\epsilon_{n\downarrow}$ are two diagonal elements of $\boldsymbol{\epsilon}_n$, where $\epsilon_{n\sigma}$ corresponds to the on-site energy. For a perfect ring $\epsilon_{n\sigma}$'s are constant and we set them to zero without loss of any generality. On the other hand, for a random disordered ring $\epsilon_{n\sigma}$'s ($\epsilon_{n\uparrow} = \epsilon_{n\downarrow}$) are chosen randomly from a 'Box' distribution function of width W within the range $-W/2$ to $W/2$. As numerical results strongly depend on disordered configurations, we take the average over a large number of such distinct configurations.

To analyze the unconventional behavior of electron transport we need to calculate current corresponding to each eigenstates along with net current for a particular electron filling. The current carried by m -th eigenstate is obtained from the following relation²³

$$\begin{aligned} I_m = & \frac{2\pi t i e}{N h} \sum_n (a_{n,\uparrow}^{m*} a_{n+1,\uparrow}^m e^{-i\theta} + a_{n,\downarrow}^{m*} a_{n+1,\downarrow}^m e^{-i\theta} + h.c.) \\ & - \frac{2\pi \alpha e}{N h} \sum_n (e^{-i\phi_{n,n+1}} a_{n,\uparrow}^{m*} a_{n+1,\downarrow}^m e^{-i\theta} \\ & + e^{i\phi_{n,n+1}} a_{n,\downarrow}^{m*} a_{n+1,\uparrow}^m e^{-i\theta} + h.c.). \end{aligned} \quad (2)$$

Therefore, at absolute zero temperature net current carried by a ring containing N_e electrons becomes $I = \sum_{m=1}^{N_e} I_m$.

Finally, the electrical conductivity is determined by calculating Drude weight D from the relation²⁴

$$D = \frac{N}{4\pi^2} \left(\frac{\partial^2 E_0(\phi)}{\partial \phi^2} \right) \Big|_{\phi \rightarrow 0} \quad (3)$$

where $E_0(\phi)$ is the ground state energy. This parameter allows us to predict the conducting ($D = \text{finite}$) or insulating ($D \rightarrow 0$) phase of any system.

Our main concern of this work is to study the interplay between α , ϕ and W qualitatively, not quantitatively considering any specific material, and therefore, throughout the numerical calculations we fix the nearest-neighbor hopping integral t at 1 eV and measure all other energies with respect to it. The current and Drude weight are calculated in units of et/h and e^2t/h^2 , respectively, where e and h are the fundamental constants.

III. RESULTS AND DISCUSSION

Let us start with Fig. 2 where the variation of current I as a function of α is shown for a 80-site half-filled ($N_e = 80$) ring. Three different cases, depending on ϕ , are taken into account and in each case we present

the results of both ordered and random disordered rings. For a sufficiently low value of ϕ (viz, $\phi = 0.001$) current in the ordered ring increases monotonically, without showing any oscillation, with α . While, anomalous oscillations with increasing peak heights are observed in the disordered ring (see Fig. 2(a)). Most notably we see that for a wide α -window current in the disordered ring becomes much higher compared to the perfect one, and

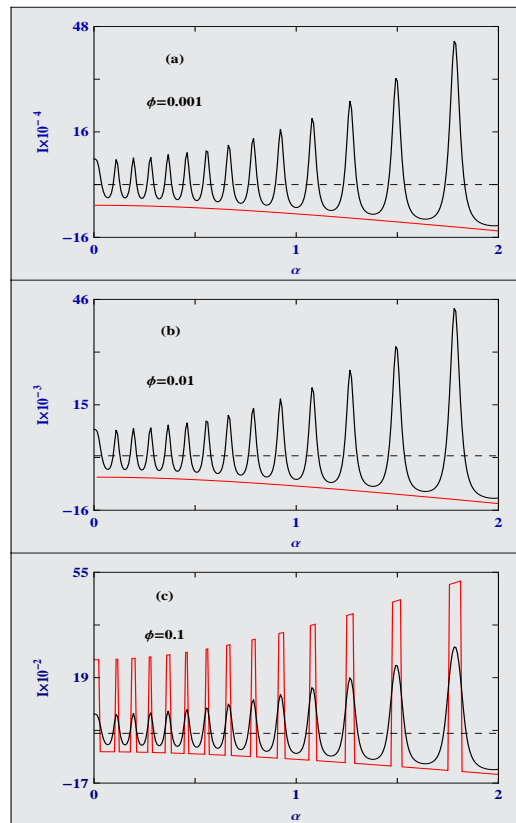


FIG. 2: (Color online). Dependence of current I on α at three typical fluxes for a 80-site ring considering $N_e = 80$. The red and black curves correspond to the perfect and random disordered ($W = 0.5$) rings, respectively. The dashed horizontal line represents the line of zero current.

the height of individual peak and its width get enhanced with increasing α . Exactly identical scenario, apart from greater current amplitude, also persists when the flux ϕ moves to 0.01 (see Fig. 2(b)). This unconventional behavior i.e., appearance of much higher current in a disordered ring than a perfect one for several α -windows disappears with increasing ϕ which is presented in Fig. 2(c). Here, the current in the ordered ring is always higher for any α -window than the disordered case and this conventional behavior remains unchanged for any other higher values of flux ϕ . Additionally, we get oscillating nature of current in ordered case (not appeared in lower fluxes), where sharp jumps between positive and negative currents are observed, unlike the disordered ring which always exhibits a smooth variation over α (black

line). This oscillating nature can be implemented by analyzing the variation of ΔE_0 as a function of α , where $\Delta E_0 = E_0(\phi_{\text{typ}} + \Delta\phi) - E_0(\phi_{\text{typ}})$ with $\Delta\phi \rightarrow 0_+$ (here we choose $\Delta\phi = 0.125/16$). For this case $\phi_{\text{typ}} = 0.1$. Using this ΔE_0 , persistent current can be calculated through the relation $-\Delta E_0/\Delta\phi$ at $\phi = \phi_{\text{typ}}$ which is the conventional prescription⁶ of determining persistent current for a particular filling. Now from the variation of ΔE_0 as a function of α (presented in Fig. 3) we see that its sign alternates between positive and negative over a finite α -window. Certainly, the factor $(\Delta E_0/\Delta\phi)$ gives oscillating nature with sign reversal (red line of Fig. 2(c)) as a function of α as $\Delta\phi$ is always positive. In addition it is important to note that the widths of the positive currents are much smaller than the negative currents (though the scenario could be opposite i.e., lesser widths of negative currents than the positive ones for other fluxes). This is solely associated with the variation of ΔE_0 - α characteristics. The window widths gradually decrease with lowering magnetic flux and eventually disappear for a sufficiently low values of ϕ which results a continuous-like variation without providing any sharp jump (red lines of Figs. 2(a) and (b)). On the other hand, disorderness makes a smooth variation of ΔE_0 with respect to α (black curve of Fig. 3) yielding a continuous-like pattern (with-

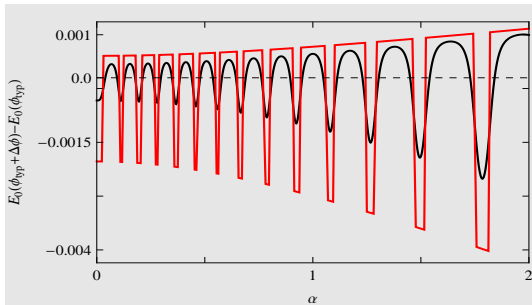


FIG. 3: (Color online). Variation of ΔE_0 as a function of α at $\phi_{\text{typ}} = 0.1$ for a 80-site ring with $N_e = 80$. The red and black curves correspond to the perfect and random disordered ($W = 0.5$) rings, respectively. Here we set $\Delta\phi = 0.125/16$.

out any sharp jump) of I - α characteristics (black lines of Fig. 2).

Regarding the oscillation in Fig. 2 it is important to note that for all the three different fluxes current exhibits almost identical (though not exactly same) oscillating feature with α . This oscillation solely depends on the variation of ΔE_0 with respect to α . For a particular ring size and fixed electron filling, the ΔE_0 - α characteristics become almost similar for all fluxes, since for any non-zero ϕ degeneracies are broken for a Rashba ring. The oscillatory pattern (i.e., separation between successive peaks) could be different for different filling factor associated with system size N . But, for a fixed N and N_e it is very hard to distinguish the separations between the peaks for different fluxes, though they are actually different which we confirm through our numerical calculations. In short, there is no proper periodicity of oscilla-

tion with α . It depends on systems size N , filling factor N_e , etc., and further detailed studies should be required to find if there is any specific periodicity.

In order to explain the atypical behavior obtained in the limit $\phi \rightarrow 0$ (i.e., higher current in disordered ring compared to the perfect one) let us focus on the spectra given in Fig. 4 where the results are computed for

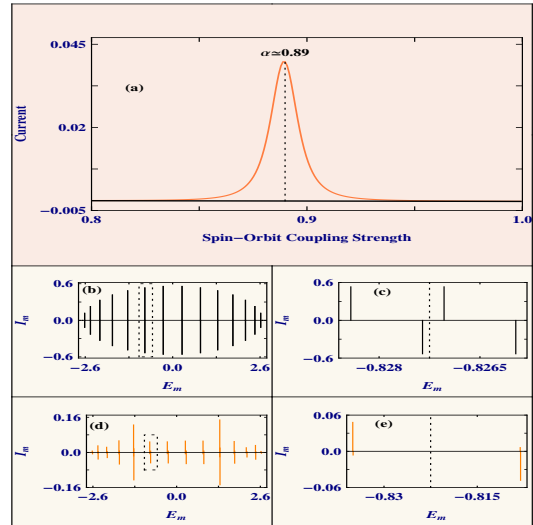


FIG. 4: (Color online). (a) Net current I for a specific α -window considering a 30-site ring with $N_e = 24$, where the black and orange curves correspond to ordered ($W = 0$) and random disordered ($W = 0.25$) rings, respectively. (b) Current I_m (vertical lines correspond to current amplitudes) carried by m -th eigenstate having eigenenergy E_m for the ordered 30-site ring. (d) Same as (b) for the disordered ($W = 0.25$) ring. All these results are worked out for $\phi = 0.001$, and the I_m - E_m spectra are drawn for the critical α ($= 0.89$) where I has a peak. The spectra (c) and (e) represent the zoomed version of the dashed framed regions of (b) and (d), respectively, containing the state currents of energy levels whose energies are close to Fermi energy E_F associated with $N_e = 24$. The dashed vertical line is passing through the gap between the highest occupied energy level and the lowest unoccupied one. Below this dashed vertical line all states (i.e., 24 states in each of the spectra (b) and (d)) are occupied which contribute to the net current, while the states above this line are empty. The current distributions of energy levels very close to Fermi energy, those essentially contribute to net current, can be clearly seen from the spectra (c) and (e). The contributions of all other occupied states having lower energies mutually cancel with each other.

a 30-site ring considering $\phi = 0.001$. In Fig. 4(a) the net currents for ordered (black line) and disordered (orange line) rings are superimposed for a specific α -window. Now choose any α , say $\alpha = 0.89$, where the net current in disordered ring is higher than the ordered one and try to analyze the individual state currents for these two rings at this typical α those are presented in Figs. 4(b) and (d). In absence of impurities successive energy levels having a tiny difference in energy eigenvalues (as $\phi \rightarrow 0$, which is responsible to break the degeneracy between $\pm k$

states) carry almost equal currents and in opposite directions (see Fig. 4(b), where vertical lines correspond to the current amplitudes). On the other hand, when we add impurities currents carried by different states become more asymmetric with respect to each other, as clearly seen from Fig. 4(d). Though all the energy levels upto Fermi energy E_F associated with electron filling $N_e = 24$ contribute to current, but the net contribution essentially comes from the energy levels having energies very close to E_F as the contributions from all other energy levels mu-

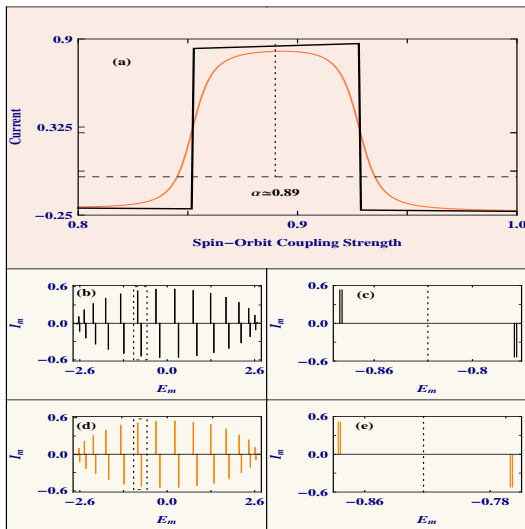


FIG. 5: (Color online). Same as Fig. 4 with $\phi = 0.1$ (moderate flux). Identical features are also observed for any other higher value of ϕ .

tually cancel with each other. For better viewing of the current distributions of energy levels close to Fermi energy, in Figs. 4(c) and (e) we present the zoomed version of the framed regions of Figs. 4(b) and (d), respectively, where the dashed vertical line separates the occupied states from the unoccupied ones. Comparing the spectra given in Figs. 4(c) and (e) we can easily understand why net current in the disordered ring is higher than the perfect one though individual state currents are much less for the previous ring. The asymmetric nature of current in the limit $\phi \rightarrow 0$ remains unchanged, yielding unconventional large current, for any kind of disordered ring (be it random or correlated) which we confirm through our detailed numerical calculations. This phenomenon can be argued physically as follows. There are three factors (SO coupling, magnetic flux and disorderness) which are responsible to control the current. In presence of ϕ and α , the current carried by individual states increases *gradually* in the case of a pure ring as we move towards the energy band centre. This is a well know phenomenon. While for the disordered ring the gradual increment of current cannot be observed as mixture of high conducting and low conducting states are there, which is even more transparent when ϕ is too small as it introduces very less current in each state. Thus, much less conduct-

ing states exhibit vanishingly small currents compared to the other comparatively higher conducting states, which makes the I_m - E_m spectrum asymmetric. This atypical nature is valid for some specific α -windows, whereas for other α -regions we get the conventional results associated with the interplay between α , ϕ and W .

From the above analysis atypical response of current in the low-field limit ($\phi \rightarrow 0$) is well understood. Now the question naturally comes why this behavior gets changed

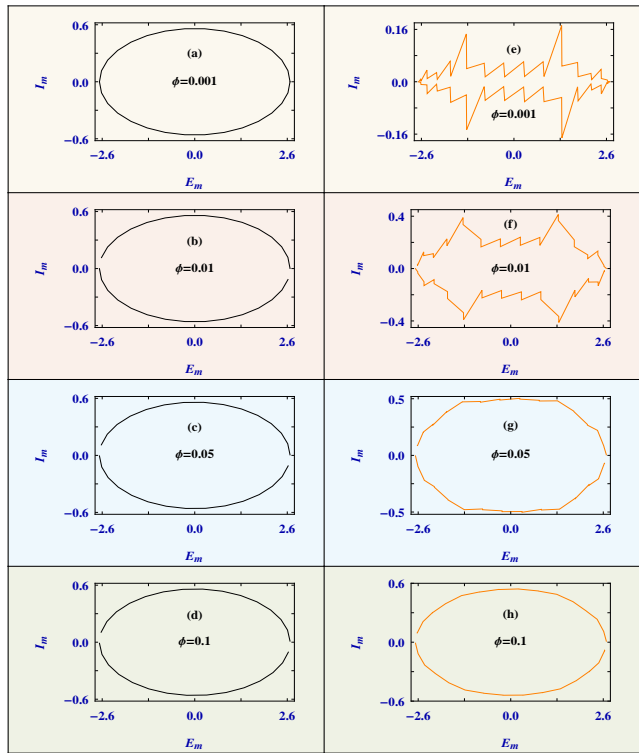


FIG. 6: (Color online). Envelope of the currents carried by individual energy levels for a 30-site ring at some typical fluxes where the 1st and 2nd columns correspond to the ordered ($W = 0$) and random disordered ($W = 0.25$) rings, respectively. All positive currents carried by different states are connected by a line to get one envelope along the positive side, and similar prescription is given to get another envelope along the negative side of individual spectrum.

with increasing ϕ , providing higher current in a perfect ring compared to the disordered one for any α . This can be explained quite easily by studying currents carried by distinct energy levels for both ordered and disordered cases. The results are shown in Fig. 5. For moderate ϕ ($\phi \approx 0.1$ or any higher value) all states carry much higher current compared to $\phi \rightarrow 0$ both for ordered and disordered cases (Figs. 5(b) and (d), respectively). The state currents for the perfect ring as usual symmetric with respect to each other, but due to enhancement of currents as a result of ϕ disordered ring also exhibits quite symmetric patterns in the I_m - E_m spectrum (Fig. 5(d)). Here it is interesting to note that pairwise successive energy levels carry currents in opposite directions which is

more transparent from the zoomed version of the framed regions as placed in Figs. 5(c) and (e), unlike the case of low-flux limit where successive energy levels carry currents in opposite directions (Figs. 4(c) and (e)). Therefore, for a particular filling, a disordered ring exhibits smaller current than an ordered one, since for the later case individual state currents are always higher.

From the spectra Figs. 4 and 5 we can understand that a transition of I_m-E_m spectrum from asymmetric to symmetric nature takes place with the increment of magnetic flux ϕ . In order to visualize this transition with finer resolution in Fig. 6 we present the envelop of the currents carried by individual energy levels at some typical fluxes ranging from extremely low to a moderate one where the first and second columns correspond to the perfect and disordered rings, respectively. It is observed that in the limit of zero magnetic flux positive and negative envelops are highly asymmetric for the disordered ring and this asymmetric nature gradually decreases with increasing ϕ . Eventually the asymmetry almost disappears for the moderate magnetic flux. On the other hand, perfect ring always exhibits symmetric envelops as expected. From these results it can be emphasized that the interplay between α , ϕ and W is really very interesting and important too which has not been critically discussed before, to the best of our concern.

Finally, to substantiate more precisely the anomalous low-field response, in Fig. 7 we present the variation of electrical conductivity (viz, Drude weight D) as a function of α both for ordered and disordered cases. Three different types of disordered rings, random, Fibonacci and Thue-Morse (TM) are taken into account in order to establish the invariant nature of atypical response on disorderness in the limit $\phi \rightarrow 0$. The results are presented in Figs. 7(a), (b) and (c), respectively, and in each case $D-\alpha$ spectrum of ordered ring (green curve) is superimposed. Both these two correlated disordered rings (Fibonacci and Thue-Morse) are constructed using two primary lattices, (say) A and B , following proper inflation rules. For the Fibonacci sequence²⁵ it is $A \rightarrow AB$ and $B \rightarrow A$, while for the other (TM) case²⁶ it becomes $A \rightarrow AB$ and $B \rightarrow BA$. Depending on A -type or B -type atomic site $\epsilon_{n\sigma}$ can be simply written as ϵ_A or ϵ_B , as sites are non-magnetic. From the spectra (Fig. 7) it is observed that Drude weight exhibits pronounced oscillation in presence of disorder, similar to current oscillation in the limit $\phi \rightarrow 0$ (black lines of Figs. 2(a) and (b)), and this pattern does not change with disorderness i.e., whether it is correlated or random. On the other hand, for the ordered case a continuous variation with increasing magnitude of conductivity is obtained, obeying the earlier current analysis (red lines of Figs. 2(a) and (b)). Interestingly we see that for wide ranges of α electrical conductivity in disordered ring becomes much higher compared to the perfect one, and this strange behavior is fully consistent with our previous current analysis for $\phi \rightarrow 0$.

At the end, it is important to note that a disordered

ring can provide metal-to-insulator transition at multiple values of α which is clearly visible from the oscillating nature of $D-\alpha$ curve (red line of Fig. 7). Thus the present system can be utilized as a controlled switching device, since we can tune α externally, and certainly it gives a high impact in the present era of nanotechnology.

The results studied here have been worked out for a Rashba ring. All these features remain exactly invariant if one takes a Dresselhaus ring instead of the Rashba one.

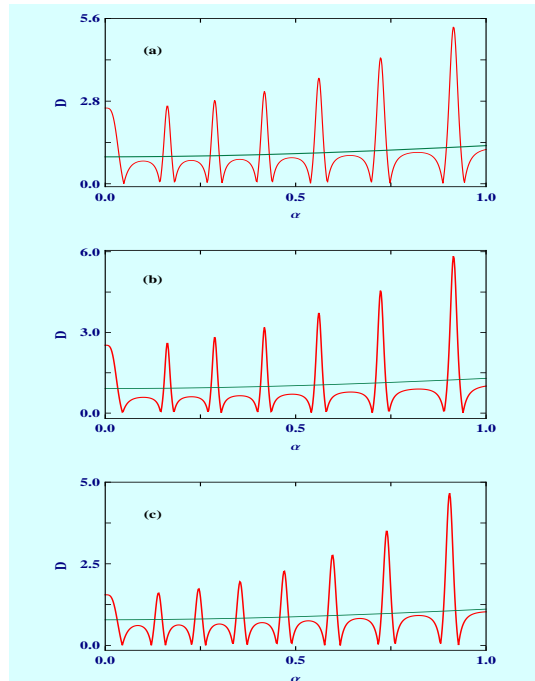


FIG. 7: (Color online). $D-\alpha$ characteristics (red line) of three different types of disordered rings. (a) Random disordered ($W = 0.5$) ring with $N = 55$, $N_e = 54$; (b) 9th generation ($N = 55$) Fibonacci ring ($\epsilon_A = -\epsilon_B = 0.5$) with $N_e = 54$ and (c) 7th generation ($N = 64$) TM ring ($\epsilon_A = -\epsilon_B = 0.25$) with $N_e = 64$. In each case $D-\alpha$ curve (green line) for ordered ring ($W = 0$ or $\epsilon_A = \epsilon_B = 0$) is superimposed.

In presence of Dresselhaus SO coupling the Hamiltonian of the ring looks like,

$$\begin{aligned} \mathcal{H} = & \sum_n c_n^\dagger \epsilon_n c_n + \sum_n \left(e^{i\theta} c_{n+1}^\dagger t c_n + e^{-i\theta} c_n^\dagger t^\dagger c_{n+1} \right) \\ & + \sum_n \beta \left[c_{n+1}^\dagger (i\sigma_y \cos \varphi_{n,n+1} + i\sigma_x \sin \varphi_{n,n+1}) \right. \\ & \left. e^{i\theta} c_n + h.c. \right] \end{aligned} \quad (4)$$

where β measures the strength of Dresselhaus SO coupling. Inspecting the Hamiltonians for Rashba and Dresselhaus rings (Eq. 1 and Eq. 4) it is seen that these two Hamiltonians are connected via a unitary transformation $U^\dagger \mathbf{H} U = \mathcal{H}$, where $U = (\sigma_x + \sigma_y)/\sqrt{2}$ is the unitary matrix. Therefore, any eigenstate $|\psi_m\rangle$ of the Rashba ring can be written in terms of the eigenstate $|\psi'_m\rangle$ of the Dresselhaus one where $|\psi_m\rangle = U|\psi'_m\rangle$.

This immediately gives the current for the Dresselhaus ring: $I_m(\text{for } \mathcal{H}) = \langle \psi'_m | \mathbf{I} | \psi'_m \rangle = \langle \psi_m | U^\dagger \mathbf{I} U | \psi_m \rangle = \langle \psi_m | \mathbf{I} | \psi_m \rangle = I_m(\text{for } \mathbf{H})$. Therefore, the nature of the current carrying states for the Rashba ring becomes exactly identical to that of the Dresselhaus ring, and similar argument is also true for other measurable quantities.

Though our analysis is purely theoretical, but all these features can be verified experimentally since fabrication of small quantum ring with few electrons (even less than ten electrons²⁷) is possible with recent technological advancements, and, the magnetic field required to produce such low fluxes (i.e., $\sim 0.001\phi_0$) is also within the experimental range. It is around 0.52 Tesla for a 100-site normal metal ring with lattice spacing $a = 1\text{\AA}$, which can definitely be achieved in realistic situation.

IV. CLOSING REMARKS

In the present work we have investigated an unconventional behavior of electron transport in a 1D disordered

mesoscopic ring subjected to Rashba SO coupling. It provides a sufficiently large current compared to a fully perfect ring in the limit $\phi \rightarrow 0$ which has been analyzed by calculating individual state currents through second-quantized approach. The atypical response has been further confirmed by studying Drude weight D . Like current, it also exhibits strange oscillations and for wide regions of α electrical conductivity in a disordered ring becomes much higher than a perfect ring. Most notably we have seen that this atypical behavior is independent of the disorderness which we have verified by considering three different types of disordered rings. Finally, a possibility of getting metal-to-insulator transition at multiple values of α has been discussed that can be utilized for selective switching action.

V. ACKNOWLEDGMENT

MP is thankful to University Grants Commission (UGC), India for research fellowship.

* Electronic address: santanu.maiti@isical.ac.in

- ¹ M. Büttiker, Y. Imry, and R. Landauer, Phys. Lett. A **96**, 365 (1983).
- ² G. Bouzerar, D. Poilblanc, and G. Montambaux, Phys. Rev. B **49**, 8258 (1994).
- ³ T. Giamarchi and B. Sriram Shastry, Phys. Rev. B **51**, 10915 (1995).
- ⁴ A. Schmid, Phys. Rev. Lett. **66**, 80 (1991).
- ⁵ H. F. Cheung, E. K. Riedel and Y. Gefen, Phys. Rev. Lett. **62**, 587 (1989).
- ⁶ H. F. Cheung, Y. Gefen, E. K. Riedel, and W. H. Shih, Phys. Rev. B **37**, 6050 (1988).
- ⁷ G. Montambaux, H. Bouchait, D. Sigeti and R. Friesner, Phys. Rev. B **42**, 7647(R) (1990).
- ⁸ A. Kambili, C. J. Lambert, and J. H. Jefferson, Phys. Rev. B **60**, 7684 (1999).
- ⁹ S. K. Maiti, J. Chowdhury and S. N. Karmakar, J. Phys.: Condens Matter **18**, 5349 (2006).
- ¹⁰ S. K. Maiti and A. Chakrabarti, Phys. Rev. B **82**, 184201 (2010).
- ¹¹ S. K. Maiti, M. Dey, S. Sil, A. Chakrabarti, and S. N. Karmakar, Europhys. Lett. **95**, 57008 (2011).
- ¹² P. J. Monisha, I. V. Sankar, S. Sil, and A. Chatterjee, Sci. Rep. **6**, 20056 (2016).
- ¹³ J. Splettstoesser, M. Governale, and U. Zülicke, Phys. Rev. B **68**, 165341 (2003).
- ¹⁴ L. P. Lévy, G. Dolan, J. Dunsmuir, and H. Bouchait, Phys.

- Rev. Lett. **64**, 2074 (1990).
- ¹⁵ V. Chandrasekhar, R. A. Webb, M. J. Brady, M. B. Ketchen, W. J. Gallagher, and A. Kleinsasser, Phys. Rev. Lett. **67**, 3578 (1991).
- ¹⁶ D. Mailly, C. Chapelier, and A. Benoit, Phys. Rev. Lett. **70**, 2020 (1993).
- ¹⁷ R. Deblock, R. Bel, B. Reulet, H. Bouchait and D. Mailly, Phys. Rev. Lett. **89**, 206803 (2002).
- ¹⁸ B. Reulet, M. Ramin, H. Bouchait and D. Mailly, Phys. Rev. Lett. **75**, 124 (1995).
- ¹⁹ H. Bluhm, N. C. Koshnick, J. A. Bert, M. E. Huber, and K. A. Moler, Phys. Rev. Lett. **102**, 136802 (2009).
- ²⁰ Y. A. Bychkov and E. I. Rashba, JETP Lett. **39**, 78 (1984).
- ²¹ G. Dresselhaus, Phys. Rev. **100**, 580 (1955).
- ²² L. Meier, G. Salis, I. Shorubalko, E. Gini, S. Schön, and K. Ensslin, Nature Physics **3**, 650 (2007).
- ²³ M. Patra and S. K. Maiti, Eur. Phys. J. B **89**, 88 (2016).
- ²⁴ W. Kohn, Phys. Rev. **133**, A171 (1964).
- ²⁵ G. J. Jin, Z. D. Wang, A. Hu, and S. S. Jiang, Phys. Rev. B **55**, 9302 (1997).
- ²⁶ H. Lei, J. Chen, G. Nouet, S. Feng, Q. Gong, and X. Jiang, Phys. Rev. B **75**, 205109 (2007).
- ²⁷ U. F. Keyser, C. Fühner, S. Borck, R. J. Haug, M. Bichler, G. Abstreiter, and W. Wegscheider, Phys. Rev. Lett. **90**, 196601 (2003).